RESEARCH PAPER

Acta Neurobiol Exp 2025, 85: 1–15 DOI: 10.55782/ane-2025-2660



Effects of chronic cuff electrode implantation and stimulation of the rat tibial nerve: ultrastructural analysis of myelinated axons and their microenvironment

Olga Gajewska-Woźniak^{1,2*}, Julita Czarkowska-Bauch², Andrzej A. Szczepankiewicz³, Małgorzata Skup²

¹ Laboratory of Molecular Basis of Behavior, Nencki Institute of Experimental Biology PAS, Warsaw, Poland ² Group of Restorative Neurobiology, Nencki Institute of Experimental Biology PAS, Warsaw, Poland ³ Laboratory of Electron Microscopy, Nencki Institute of Experimental Biology PAS, Warsaw, Poland *Email: o.gajewska@nencki.edu.pl

Numerous experimental data point to therapeutic effects of electrical stimulation of peripheral nerves. Stimulation of low-threshold proprioceptive afferents to motoneurons (MNs) innervating the ankle extensor muscles of the rat increases glutamatergic Ia MN inputs and spinal and muscle expression of neurotrophin-3, instrumental for proprioceptive afferent-MN connections. We aimed to examine morphological consequences of the cuff electrode implanted around the tibial nerve used for chronic stimulation which may cause unwanted effects through its long-lasting contact with the nerve. We addressed also the questions if stimulation of low-threshold proprioceptive afferents may contribute to neural damage, affect capillary vessels and macrophage morphology reflecting functional state of the nerve. Their consequences on axonal and nerve ultrastructure have not been previously evaluated. To examine the effect of cuff electrodes and of 7-day low-threshold stimulation applied in the 4th week post-implantation on the tibial nerve, electrodes were implanted bilaterally, and a stimulation was added unilaterally. Non-implanted group was the control. The counts of myelinated axons, their cross-sectional area (>1 µm²) and circularity were measured on photomicrographs captured with use of light microscope from semi-thin Epon sections stained with toluidine blue. Ultrastructural observations with TEM included myelin, axoplasm, Remak fibers, blood vessels, macrophages and fibroblasts. Four weeks after implantation of the cuff, the mean cross-sectional area of the nerve, and counts, area and diameter of the myelinated fibers were lower compared to control. The largest fibers located in the external parts of the main nerve branches and dispersed in small branches were changed the most. No significant difference in either parameter between unstimulated (NS) and stimulated (S) nerve was found. Axons in Remak bundles were dispersed comparably in NS and S nerves. Thinly myelinated fibers demonstrating features of demyelination with remyelination were identified. We provide evidence that long-lasting presence of the cuff electrode is not neutral for nerve structure, causing mild shrinkage of large myelinated axons and impairment of organization of unmyelinated fibers. Since we demonstrated that low-threshold proprioceptive stimulation of the tibial nerve results in a stable Hoffmann reflex and induces synaptic plasticity by increasing glutamatergic input to MNs, we conclude that the applied protocol maintains an adequate margin of safety.

Key words: axon degeneration and plasticity, motor axons, Remak fibers, Schwann cells, axon shrinkage, epineural swelling, demyelination

INTRODUCTION

Numerous experimental data point to therapeutic effects of electrical stimulation of peripheral nerves. There is an accumulation of data on potential modulation of proprioceptive input to α -motoneurons (MNs) by means of electrical stimulation of low-threshold muscle afferents. The Hoffmann (H) reflex, an electrical analog of monosynaptic stretch reflex, is a useful tool to control the strength of stimulation addressed predominantly to Ia afferents. When combined with operant conditioning, this method allows teaching animals to increase an amplitude of H-reflex of ankle extensor MNs, as shown by Wolpaw's group (Chen et al., 2010). It was also shown to compensate for the asymmetrical deficit of locomotion, which developed after unilateral lesion of the lateral column in the spinal cord (Chen et al., 2006). Importantly, in trained animals, an increase of H-reflex was found to be persistent, and the effect was observed up to 100 days after termination of the operant conditioning (Chen et al., 2014). These observations indicate that profound beneficial plasticity of the spinal cord may be achieved by proprioceptive stimulation of the nerve.

Also our previous work showed that one week of stimulation of low-threshold fibers in the tibial nerve of the rat, increasing monosynaptic input to the ankle extensor motoneurons (MNs), causes an increase of expression of neurotrophin-3 (NT3) in the spinal cord and soleus muscle (Gajewska-Woźniak et al., 2013). In axotomized medial gastrocnemius nerve NT-3 administration not only prevents a decline of the EPSP amplitude but also promotes its recovery (Mentis et al., 2010). These effects indicate that NT-3 upregulation is a good predictor of structural synaptic plasticity, which was confirmed by increased number and aggregate volume of direct glutamatergic (VGluT1 IF) and indirect cholinergic (VChAT IF) inputs to lateral gastrocnemius (LG) MN perikarya (Gajewska-Woźniak et al., 2016). However, on the sham-stimulated side the number of VGLUT1 IF terminals was decreased compared to that in the control group. This observation suggested that the cuff electrodes implanted around the tibial nerves could cause some damage to the afferent fibers. If so, electrical stimulation would lead rather to the reversal of impairment in the stimulated limb pointing to successful recovery processes after stimulation of these afferents. The sources and morphological characteristics of presumed impairment and recovery in this model have not been identified.

Risk of injury associated with implantation procedure and nerve compression was described in early papers, showing local demyelination after pneumatic tourniquet application (Ochoa et al., 1971). Acute, sev-

eral hours nerve compression in rabbits induced an epineurial edema by increasing the permeability of the epineurial vessels while compression of prolonged duration caused injury also to the endoneurial vessels, leading to intrafascicular edema (Rydevik & Lundborg, 1977). Surgical implantation can injure nerve fibers or fascicles directly, resulting in various degrees of functional impairment. Also electrical stimulation itself is considered to be an element of potential nerve injury, shown in the cat to be dependent on intensity and temporal pattern of the stimulation (Agnew et al., 1989). Many electrode designs developed to study nerve activity are suitable for relatively large nerves (e.g., 3 mm diameter sciatic nerve of the cat) but are difficult to scale down for use with small, delicate nerves of the rat (e.g., 0.5-1 mm diameter individual muscle- and cutaneous nerve branches) (Stein et al., 1977a; Sauter et al., 1983). The cuff electrodes implanted around the nerve used by us and their modifications are often used for chronic stimulation and recording of peripheral nerve activity in cats (Loeb & Peck, 1996; Fisher et al., 2014) but consequences of their long-lasting contact with the nerves in rats have not been previously evaluated. Of primary relevance is the mechanical restriction by the electrode, which may exert pressure and constriction on the nerve, described for the helical electrodes implanted on the peroneal nerve of cats (Agnew et al., 1989). Damage can also be produced by wires rubbing the nerve surface or tethering the implanted nerve. Scarfing reaction attaches electrodes to the nerve and stabilizes the contact but attachment to the neighboring muscles produces a risk of traction upon the nerve during limb movement and muscle contraction.

The risk factors of surgical exposure, mechanical manipulation and contact with electrode material produced when a cuff is implanted around the rat tibial nerve long-term prompted us to undertake this study. We aimed to evaluate the effects of implantation and the impact of several daily low-threshold electrical stimulations repeated for 7 days on morphological features and ultrastructure of endoneurium and epineurium in the implanted nerves. The number of myelinated fibers was measured and morphology of Remak bundles, features of microvasculature, epineurium, macrophages and fibroblasts were evaluated.

We show that one month presence of the cuff around the rat tibial nerve causes mild, focal demyelination of large diameter axons and a loosening of some bundles of unmyelinated fibers. These changes are accompanied by the enlargement of epineurium, with numerous blood vessels retaining the structural characteristics of an impermeable blood nerve barrier. Low-threshold proprioceptive stimulation of the nerve applied with 3-week delay does not change the mor-

phological characteristics of the nerve which may be of clinical relevance.

METHODS

Animals

The experiments were carried out on 12 adult, male, Wistar rats supplied by Medical University of Bialystok, Poland. Rats weighed 230-320 g at the beginning of the experiment.

The animals were bred in the animal house at the Nencki Institute of Experimental Biology in Warsaw, Poland. They were given free access to water and pellet food and were housed under standard humidity and temperature conditions on a 12 h light/dark cycle. Rats were housed in groups of 4-6 until implantation and were housed individually afterwards.

Experimental protocols involving animals, their surgery and care were approved by the First Local Ethics Committee in Warsaw (no 535/2014), in compliance with the guidelines of the European Community Council Directive 2010/63/UE of 22 September 2010 on the protection of animals used for scientific purposes.

The animals were divided into two groups: control, without electrode implantation (N=6) and experimental, subjected to bilateral implantation of cuff electrodes on the tibial nerve and EMG electrodes into soleus (Sol) muscle. Animals with implanted electrodes received unilateral electrical stimulation of low-threshold muscle afferents in that nerve (N=6). Both groups of rats received bilateral intramuscular tracer injections to the LG to identify Ia glutamatergic inputs to LG MNs (Gajewska-Woźniak et al., 2016).

Implantation of electrodes, retrograde tracing of motoneurons, and post-surgery care

Procedure and the surgery necessary for implantation of the electrodes and tracer injections were the same as those described in detail in our former articles (Gajewska-Woźniak et al., 2013; 2016; Grycz et al., 2019). All steps were performed in the surgery room, under aseptic conditions. The animals were given subcutaneous injection of Butomidor (Butorfanolum, Richter Pharma, 1.5 mg/300 g body wt.) as a premedication and then were anesthetized with isoflurane (Aerrane, Baxter, 1-2.5% in oxygen) via a facemask. The skin on the lower part of the back and on hind paws was shaved and disinfected with alcohol and 3% hydrogen peroxide. A connector plug for the electrodes was sewn to the muscles and ligaments over the vertebrae. The

electrodes were drawn subcutaneously from the connector plug to the tibial nerves and soleus (Sol) muscles to be implanted (Fig. 1). Bipolar cuff electrode was performed as described by (Loeb & Peck, 1996). A pair of stainless-steel multi stranded Teflon-coated fine-wire electrodes (Bergen Cable Technologies Inc.) spaced apart by ~4 mm was sewn into a silicone rubber cuff (diameter: 5 mm, length: 6 mm). The internal diameter of the cuff electrode was more than 2-fold bigger than that of the tibial nerve. The popliteal fossae were opened and approximately 1 cm- long fragment of the tibial nerve was separated from the common peroneal and sural branches. The cuff electrode was implanted carefully around the tibial nerve and closed with attached sutures.

A pair of Teflon-coated electrodes with 1.5 mm final bare, spaced apart by about 5 mm were implanted in the Sol muscle to record compound muscle action potentials.

Next, fluorescent tract-tracer True Blue (15 μ l of 1% aqueous solution, TB Chloride T0695, Sigma-Aldrich) was injected to the LG muscle, a close synergist of Sol, which is also innervated by tibial nerve branches and subjected to electrical stimulation via cuff electrode. That was done to avoid leakage of the tracer from the Sol muscle with EMG electrodes implanted. Hamilton microsyringe with attached 22-gauge needle was gradually advanced from the distal toward the proximal end of the muscle belly. After 5 min lasting injection the needle was left in the muscle for 3 min to avoid leakage of the dye. The injection site was cleaned and the skin was sutured.

After the surgery, Baytril (Enrofloxacinum, 5 mg/kg, s.c., Bayer) was administered over five consecutive days to prevent infection. An analgesic Tolfedine (Tolfenamic acid 4%, 4 mg/kg, s.c., Vetoquinol S.A.) was given during the 3 postoperative days. Immediately after the surgery, the rats were placed in warm cages, covered with blankets and inspected until fully awakened. Thereafter plastic collars (Harvard Apparatus) were put on each animal to protect wounds from licking, and rats were returned to individual cages with full access to food and water.

Low-threshold proprioceptive stimulation of the tibial nerve and Hoffmann reflex recording

To reduce the effects of behavioral context and ongoing motor activity on the recorded H-reflexes the rats were accustomed to being restrained in the apparatus which limited their body movements.

The monosynaptic H-reflex was elicited by electrical stimulation addressed predominantly to low-threshold

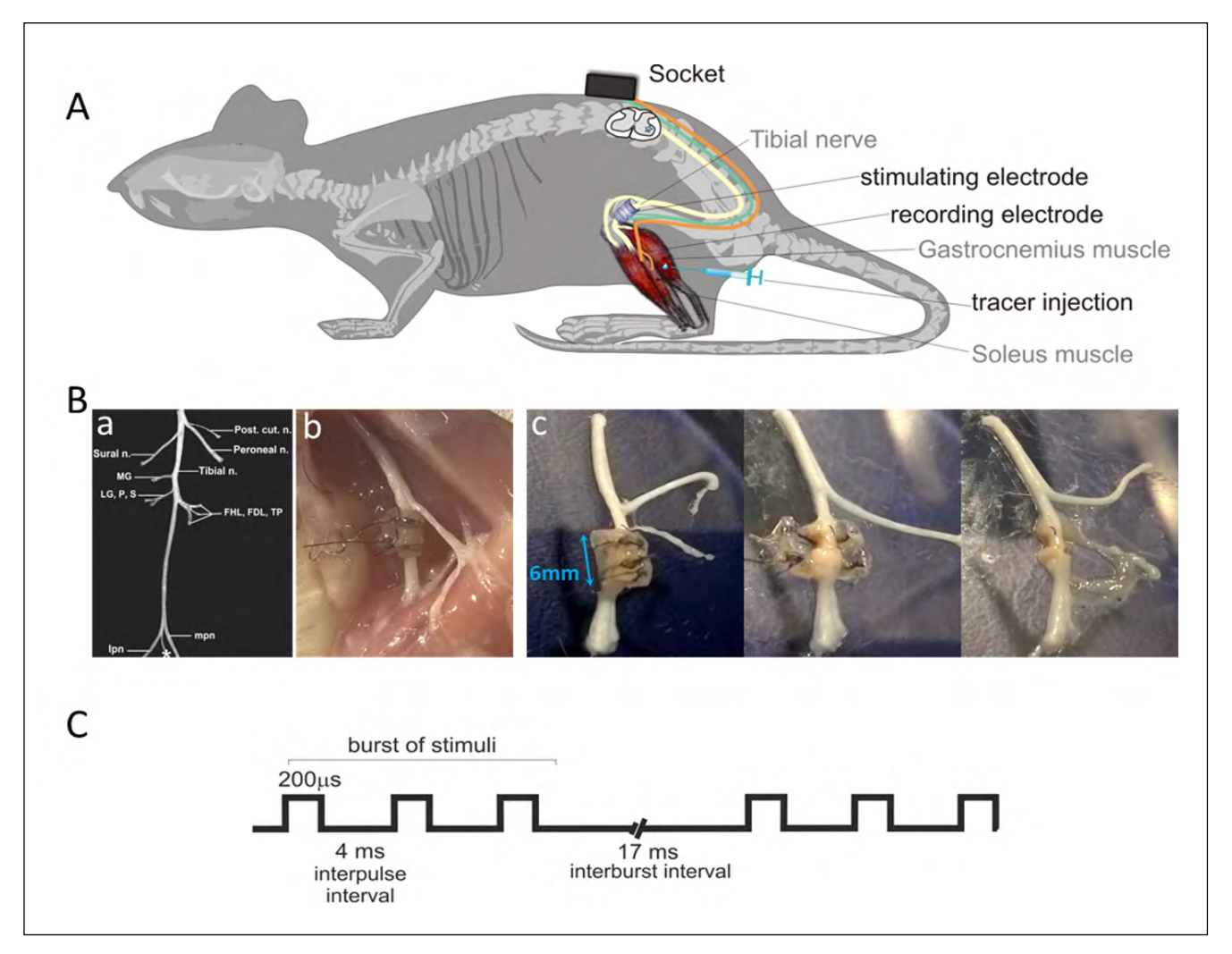


Fig. 1. (A) Experimental model, (B) Cuff electrode implantation; a. identification of the tibial nerve branches (Badia et al., 2010), b. implantation below peroneal and sural branches, c. nerve with a cuff, prior to and after cuff removal at 4 weeks post-implantation. The connective tissue is visible outside and inside the cuff, more compact in the area where the electrodes are situated. (C) Electrical stimulation paradigm applied (Gajewska-Woźniak et al., 2013; 2016).

muscle afferents (Ia group) in the tibial nerve and recorded as a compound muscle action potential in the Sol muscle (Fig. 2) as described in detail in our former article (Gajewska-Woźniak et al., 2013). The strength of stimulation was near the threshold of excitation of the motor fibers, which is higher than the one activating Ia afferents. This current elicited a fair H-reflex, since the majority of Ia fibers were already excited when the direct motor response (M) was at its threshold (Czarkowska et al., 1976). Therefore, we monitored both the H-reflexes and M-responses and corrected the current, if necessary.

Three weeks after the implantation we started unilateral stimulation of the tibial nerve. The contralateral limb served as a sham-stimulated control. Each day the experiments started and ended with testing individual

threshold current values producing the H-reflex and/ or threshold M-responses to 30 single pulses of 500 μ s duration delivered at 0.3 Hz.

The main training consisted of continuous bursts of three pulses (pulse width = $200 \mu s$ with 4 ms inter-pulse interval, Fig. 1C) delivered every 25 ms to the tibial nerve in four 20 min sessions daily for seven consecutive days. After each session the animals rested for at least 1 hour in their home cages and were rewarded with corn cookies.

The averaged data of recorded compound muscle action potentials indicated a relatively stable H-reflex at both the beginning and the end of the training (see table in Fig. 2). This suggests that the low-threshold Ia muscle afferents in the tibial nerve remained unaffected by the applied stimulation. The maximal direct

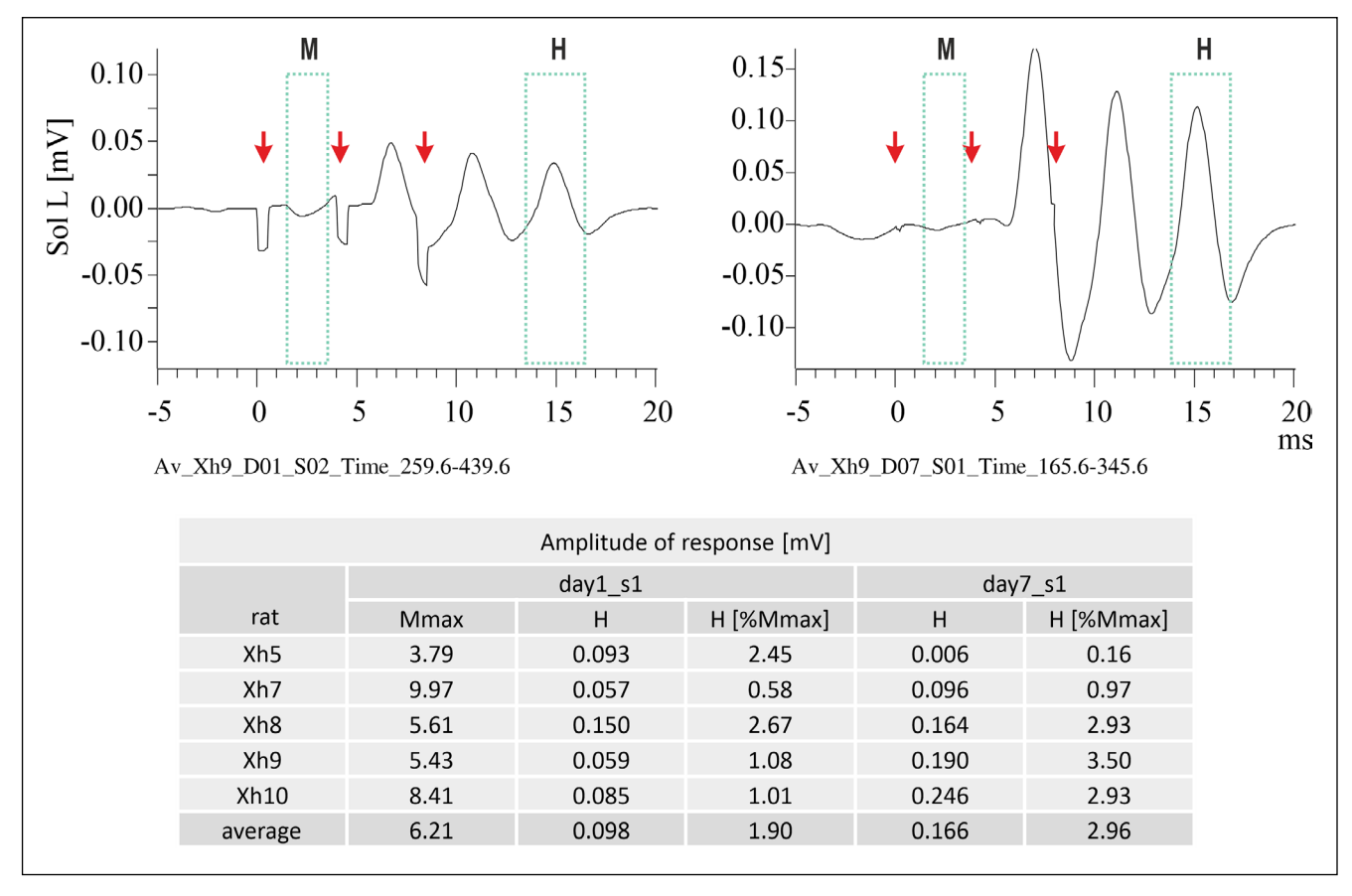


Fig. 2. An example of H- and M-waves recorded in the soleus (Sol) muscle in response to continuous bursts of 3 pulses (arrows) applied to the tibial nerve. The signals were averaged over 7200 burst repetitions (3 min of stimulation). The mean latencies for the H- and M-responses in Sol were 5.9 ms and 1.9 ms, respectively. During burst stimulation, only the first M-wave and the last H-wave (highlighted in frames) were analyzed, as they remained unaffected by overlapping responses. The accompanying table presents the amplitude values of the H-reflex on the first and last day of stimulation (s1 – first session), along with the maximal direct M-response (Mmax).

motor response (Mmax), was measured once during the experiment. Mmax represents the largest electrical response recorded from a muscle following supramaximal electrical stimulation of its motor nerve, signifying the full activation of all motor units. We used Mmax to normalize electromyographic (EMG) signals, enabling a consistent comparison of H-reflex amplitudes across individuals.

Data acquisition and analysis of electrophysiological data

Acquisition and analysis of electrophysiological data have been described in detail in our former article (Gajewska-Woźniak et al., 2013; 2016). Briefly, after amplification the analog EMG signals were fed to a CED Micro 1401 mk II interface (Cambridge Elec-

tronic Design Ltd, UK), digitized and fed to a PC. Raw EMG activity was also monitored throughout the experiment on the oscilloscopes. A Spike 2 (Cambridge Electronic Design Ltd, UK) based script was used to measure the latency, peak-to-peak amplitude, area of the H-reflex and M-response and to average these data. These results were expressed as a percentage of Mmax elicited by single-pulse stimuli and collected in each animal after the last session on the 6th day of stimulation.

Tissue processing

Within 1.5 h after the last stimulation session, the animals were anesthetized with a lethal dose of Morbital (pentobarbital 120 mg/kg body weight, intraperitoneal; Biowet Puławy) and perfused transcardially with

250 ml 0.01 M phosphate-buffered saline (pH 7.4), at room temperature, followed by 450 ml ice-cold fixative (4% paraformaldehyde, in 0.1 M phosphate buffer). Tibial nerves were isolated and postfixed in the same fixative for 1 hour at 4°C. Tissue was then cryoprotected stepwise in 10%, 20% and 30% sucrose solution in 0.1 M PB and stored at 4°C until use.

Approximately 1 mm of tissue from the middle of the cuff electrode was postfixed in 2.5% glutaraldehyde (overnight). The same level was sectioned in unoperated nerves; these nerves served as controls. Next the sampled nerves were treated with 2% osmium tetroxide to contrast and increase the retention of lipids in the tissue. After dehydrating in a series of graded ethanol, nerves were treated with uranyl acetate which produces high electron density and image contrast of membranes and nucleic acids by binding proteins and lipids with sialic acid carboxyl groups. Next, the samples were cleared in propylene oxide, and mounted in epoxy embedding medium (45359, Epoxy-Embedding Kit, Sigma Aldrich).

Transverse, semithin (0.5 μ m thick) sections were cut on an ultramicrotome (Leica, Germany), mounted on glass slides, dried and stored at RT until further processing.

Sections were subjected to myelin staining with 1.5% Toluidine Blue water solution with 0.6% sodium borate to increase medium penetration, in approximately 80°C, for 30 seconds. After several washes in ethanol, slides were air dried, mounted with DPC medium and coverslipped.

Tissue preparation for transmission electron microscopy and image sampling

Transverse ultrathin sections were prepared using an ultramicrotome (Leica, Germany) and mounted on Formvar-carbon-coated copper grids. The sections were subsequently contrasted and imaged using a transmission electron microscope (TEM), model JEM 1400 (JEOL Co., Japan, 2008). To visualize the structure and pathological features of peripheral myelin, non-myelinated axons in Remak bundles, capillary/precapillary blood vessels, macrophages and fibroblasts with TEM, images from endoneurium, perineurium and epineurium were acquired.

Counts and measurements of myelinated axons

Photographs of the tibial nerve cross-sections were taken under a light microscope Nikon Eclipse 80i (objective lens $40 \times N.A.\ 0.95$) equipped with a monochromatic CCD camera Evolution VF (Media Cybernetics, Inc.). Images were captured as a series of photos with addition-

al margin and then perfectly tiled with the use of Image-Pro Plus 7.0 (Media Cybernetics, Inc.) software. The settings of the contrast and gamma were constant at each imaging session. Exposition time and offset were adjusted if necessary to obtain the best quality images. Two cross-sections from each tibial nerve segment below the peroneal and sural muscle tributaries were chosen for morphometric analysis. Both main trunk and branches of the tibial nerve were outlined and scored using Image-Pro Premiere software. The software allows counting the number of myelinated axons in the given area and for each myelinated axon the area, diameter and circularity. The axon number and sum of the cross-sectional area of single axons were related to the cross-sectional area of the tibial nerve and its branches.

Statistical analysis

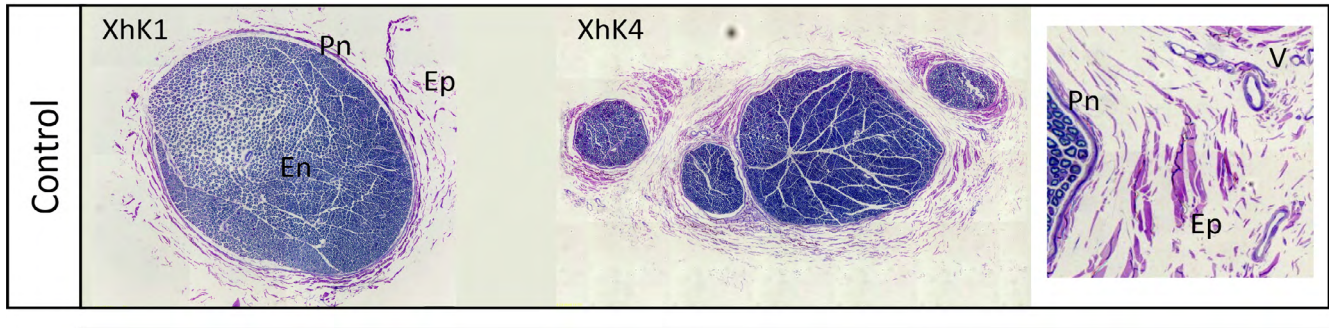
The Shapiro-Wilk test was used to verify the normality of data distribution. The homogeneity of variance in the groups was analyzed with the Levene test. The non-parametric Wilcoxon and Mann-Whitney U tests were used for comparisons of related samples and independent samples, respectively. For the analysis of changes in fiber distribution in function of the axonal cross-sectional area the Mann-Whitney U test was used. STATISTICA 13 software (StatSoft Inc. Tulsa, OK, USA) was used for data analysis. Statistical significance was set at p<0.05.

RESULTS

The effects of nerve implantation and low-threshold stimulation on the tibial nerve

In control animals a thin perineurium and epineurium, both of which were relatively poor in structural elements were observed (Fig. 3). Blood vessels, often elongated, were present along with purple-stained longitudinal fiber layers, forming the outer anatomical barrier of the peripheral nerve. The nerve fascicles were present either as a single or several bundles embedded in endoneurium and were surrounded by perineurium and epineurium (Reina et al., 2013; Reina & Sala-Blanch, 2015).

Fig. 3 shows representative images of nerves from two out of 6 control rats and 3 out of 6 rats with implanted electrodes. As shown, nerves implanted with a cuff electrode were encapsulated in a connective tissue sheath composed of inner collagenous layers and an outer matrix of cells unidentifiable under light microscope (Fig. 3, insets from Xh4, Xh5, Xh8 rats). In



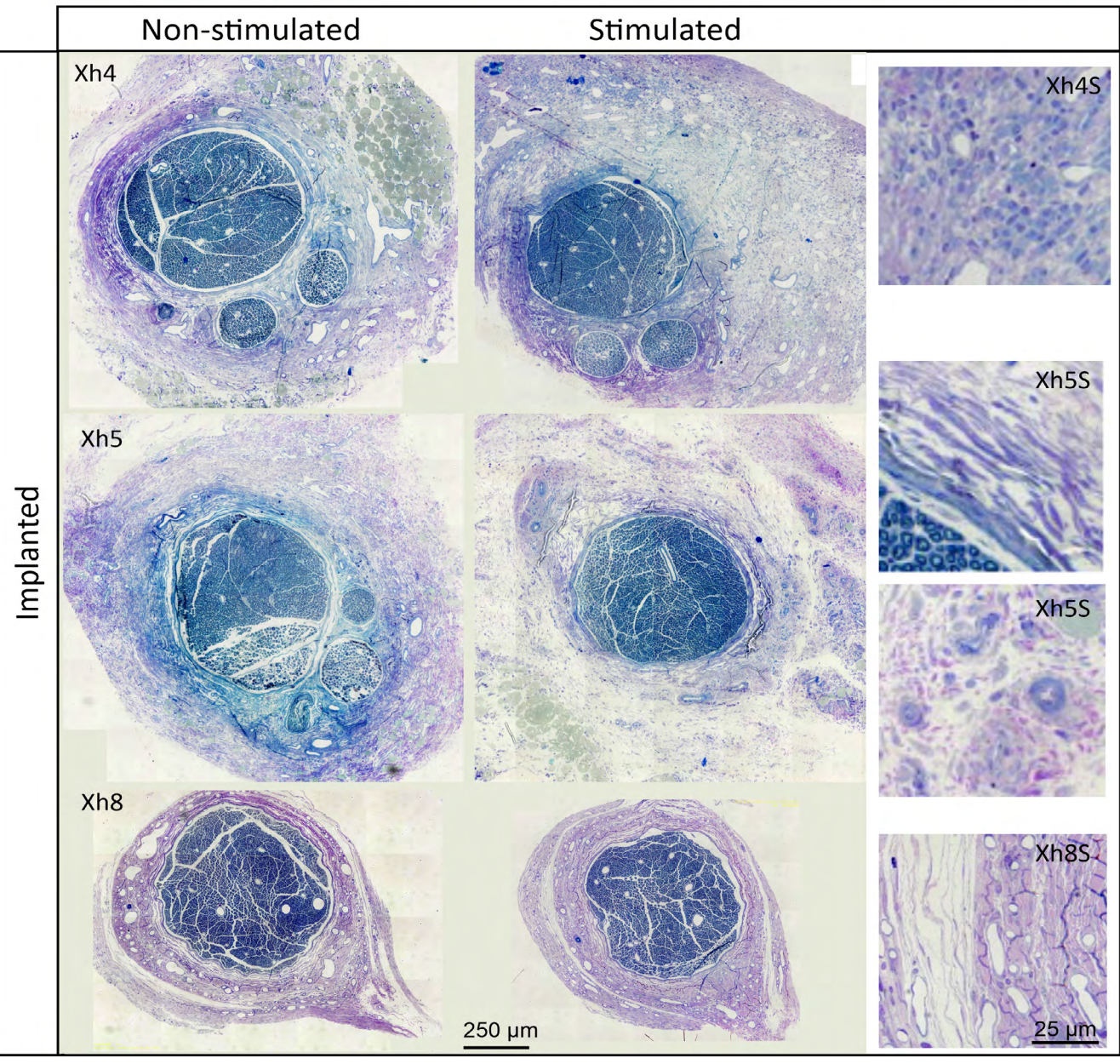
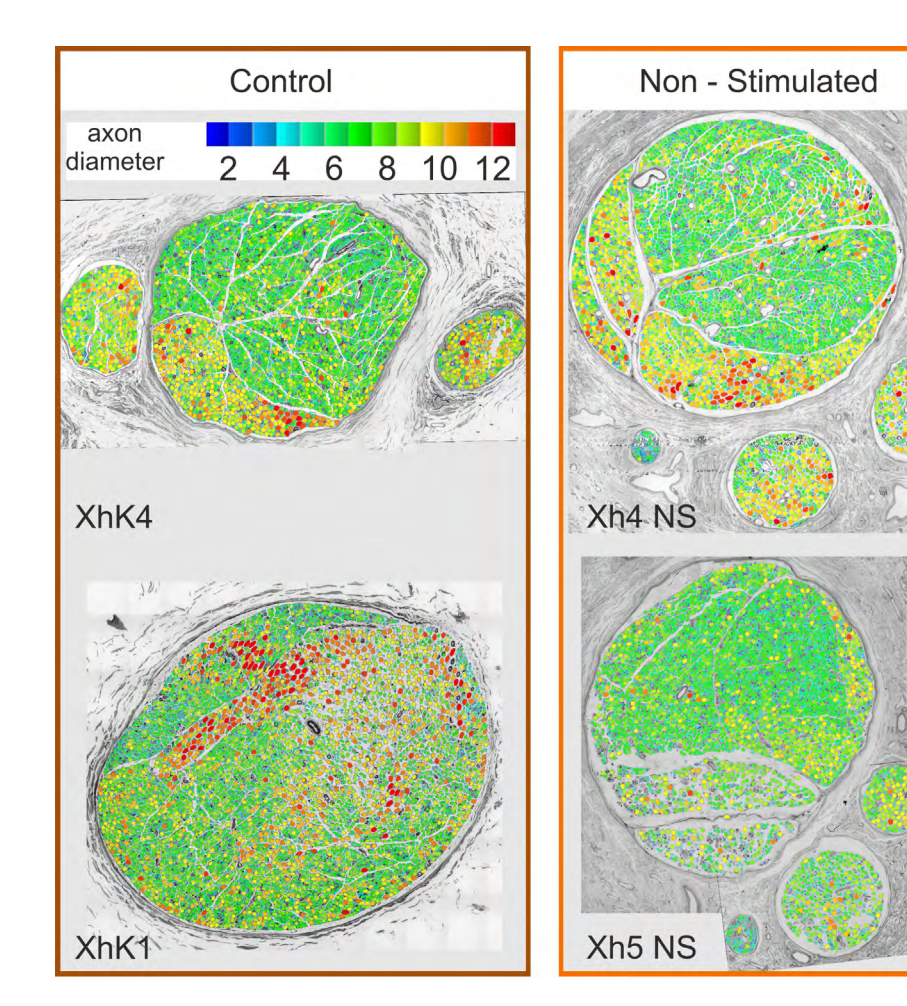


Fig. 3. The cross-sections of the rat tibial nerves, showing nerve fibers organized in fascicles, separated by intrafascicular connective tissue forming endoneurium (En). These are delimited and protected by perineurium (Pe), which was preserved in all implanted nerves. The epineurium (Ep), which forms a well-defined sheath around the secondary fascicles and encircles all peripheral nerve trunks, is marked on the images of the control nerves. Extended epineurium is shown in representative images from implanted nerves. Higher magnification of the epineurium (right) demonstrates cellularity and richly vascularized Ep of control and implanted nerves.

nerves with marked hypertrophy of the epineurium (exemplified by Xh4 and Xh5 rats) abundant connective tissue was filling the space between the nerve and the electrode. Lipid droplets, stained turquoise with toluidine blue, were detected alongside purple-stained cells, likely fibroblasts (Fig. 3, Xh5 insets). Additionally, a marked increase in vessel density in Ep was observed. From this we conclude that the surgical exposure and mobilization of 1-1.5 cm tibial nerve during implantation did not compromise the nerve vascular system and intrinsic blood supply of the nerve or contribute significantly to the presumable, mechanically induced damage. Comparison of histologic observations of NS and S nerves did not reveal differences between them, suggesting that 7 days of low-threshold stimulation neither inhibited nor enhanced the formation of the connective tissue in the epineurium and nerve microanatomy.

The effects of nerve implantation and low-threshold stimulation on the distribution of axons of different diameters in the tibial nerve in the control and cuff-implanted rats

In the tibial portion of the sciatic nerve the myelinated fibers consist about 30% of all axons, of which 6% are motor and 23% are sensory axons (Schmalbruch, 1986; Badia et al., 2010). Organization of these fibers of different sizes was assessed and is shown on the Fig. 4. The quantitative data we are reporting here concerns these two fiber populations, analyzed together (Fig. 5). The changes in the arrangement of unmyelinated sensory and sympathetic small-caliber axons ensheathed by non-myelinating Remak Schwann cells (RSCs) were a subject of TEM analysis performed in the same material and are reported later on in this paper.



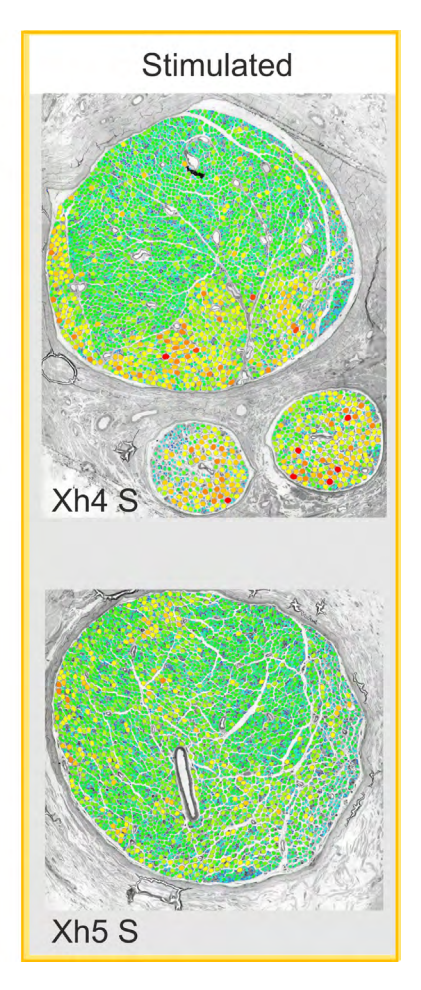


Fig. 4. The cross-sections of the rat tibial nerves, showing myelinated axons organized in fascicles. Axon diameters are color-coded with the smallest (1–5 µm) shown in blue, and the largest ones (>11 µm) shown in red. Both in control and cuff-implanted group distinguished axons of various diameters show a random pattern of distribution but the largest axons of the main tibial nerve branch tend to form clusters concentrated mainly in external fascicles.

Quantitation of the effects of nerve implantation and low-threshold stimulation on the tibial nerves at the mid-point to a cuff electrode

The average cross-sectional area of the tibial nerves in the control group was approx. $0.500~\text{mm}^2$. Four weeks after the implantation of the cuff, in 3 out of 6 animals nerves showed slightly reduced cross-sectional area under the cuff, and in the stimulated nerves there was a decline of their cross-sectional area in 4 out of 6 animals, amounting from 5% to 25% of mean area in control rats (p=0.043) (Fig. 5). The circularity of the nerve remained unchanged (0.62 +/- 0.08 in Control; 0.70 +/- 0.10 in implanted nerves). These data indicate that cuff implantation and electrical stimulation moderately affect nerve thickness not causing its deformation under the cuff.

These changes were associated with a decrease of the number of the myelinated axons. In control nerves the mean number of myelinated axons was 5713±416; it was slightly more than reported by Schmalbruch in his classical study (1986) and was within a range (per mm²) reported by (Badia et al., 2010). After implantation, axonal number was decreased slightly but significantly by 10% in NS and S groups as compared to controls (p=0.045 and p=0.008, respectively).

Axonal dimensions were similarly changed. The average cross-sectional area of axons in control nerves (38.2±4.6 μm^2) was decreased by 15% in NS and 20% in S groups (p=0.043 and p=0.014, respectively). The average diameter of axons in control nerves was 6.3±0.4 μm . It decreased by 10% in NS and S groups (p=0.043 and p=0.014, respectively). These data indicate that nerve

stimulation *per se* does not modify axonal dimensions of implanted nerves.

The changes in the mean cross-sectional area of axons followed the changes in nerve cross-sectional area as concluded from a strong positive correlation between respective values (r=0.85, p=0.030).

Changes in the size-frequency histograms of the myelinated axon diameter in the tibial nerve of control and implanted rats

Next, we carried out the analysis of frequency distribution of axons of different diameters, to answer the question which axonal population was affected the most, and how implantation affected the large axons, which would be the A α type, including α -motor and proprioceptive afferent axons. For this purpose, eleven size classes were arbitrarily distinguished in axon collections, as proposed by Szabolcs et al. (1991) (Fig. 6).

The analysis identified groups of the large axons (of diameter above 8 μ m), which in the implanted nerves were reduced in number by 30 to 50% compared to the control group. Because in the main nerve branch the largest axons of diameter over 10 μ m (Fig. 4, marked in yellow and red) were concentrated mainly in external nerve bundles, we infer that the fibers located in the external parts were the most changed. We also showed that there were more small axons (Ø 1-7 μ m) in expense of large ones (11 > Ø > 7 μ m) in cuff groups. These two observations suggest that some large axons could undergo shrinkage and appear in a different size class of myelinated axons with presumably altered properties.

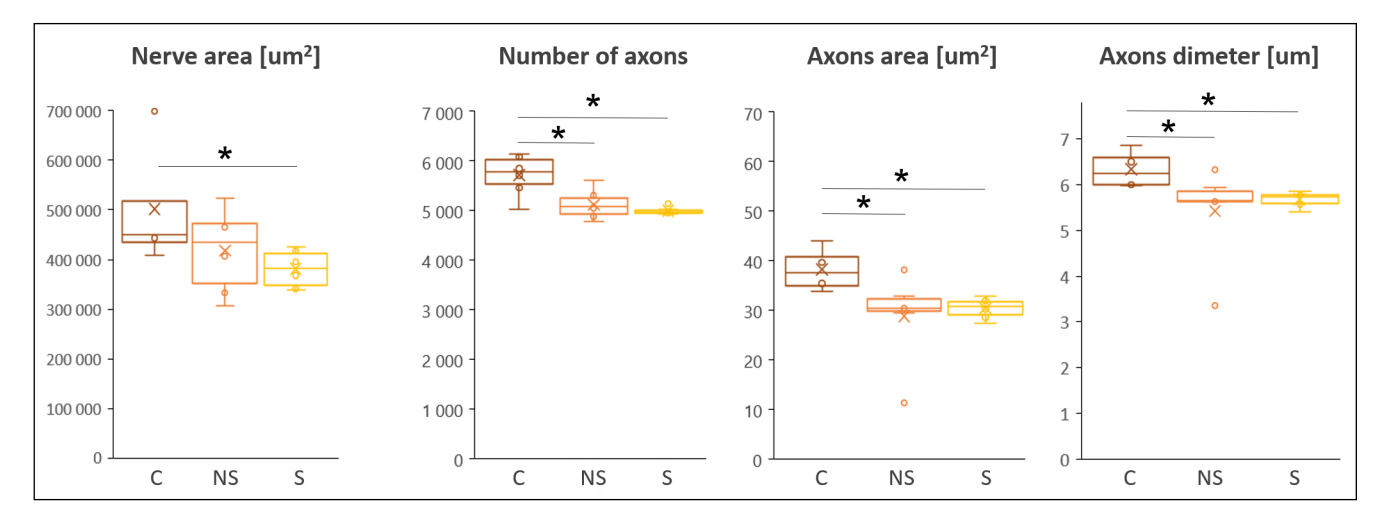


Fig. 5. The effects of nerve implantation (NS) and low-threshold stimulation (S) on the cross-sectional area of tibial nerves and on the number, diameter and cross-sectional area of myelinated axons as compared to control, non-implanted group (C). Measurements were done at the mid-point to a cuff electrode. Boxplots show quantiles (Q1 and Q3), medians (horizontal line) and means (x). Data are from 6 control and 6 implanted rats. *p<05; **p<0.01, Mann-Whitney U-test.

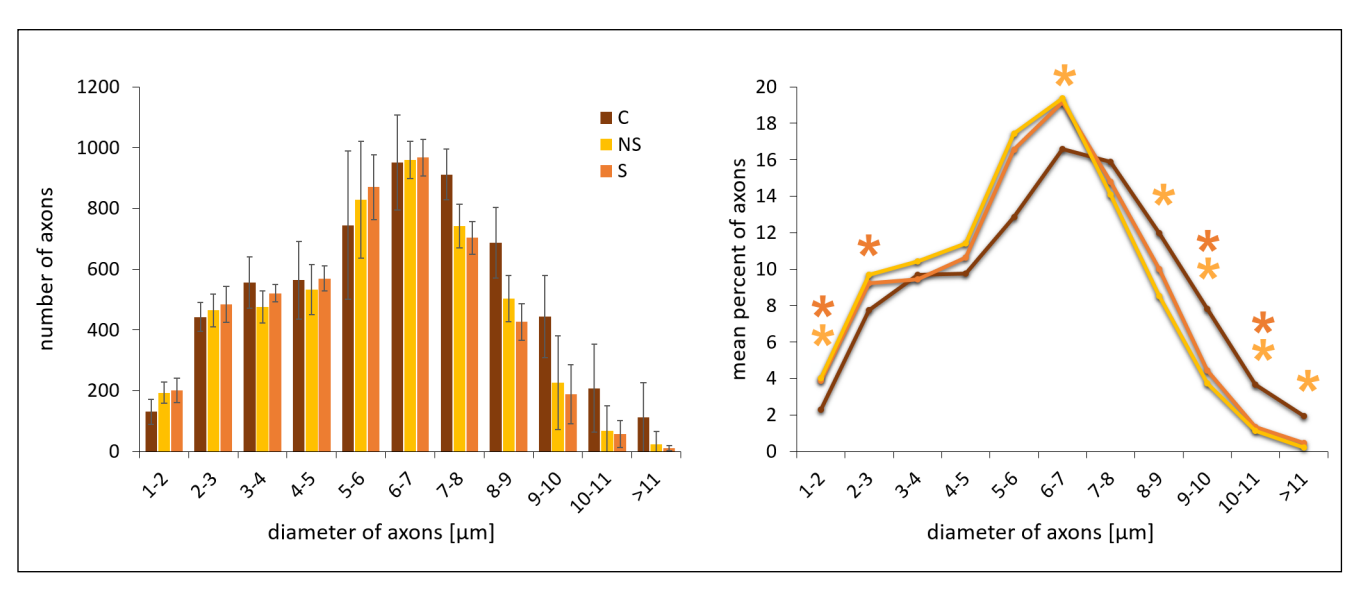


Fig. 6. Frequency distribution of myelinated nerve fibers of different diameters in Control (C) and implanted (NS, S) tibial nerve. Data on the histogram represents means +/- SD from 6 control and 6 implanted rats. *p≤0.05, Mann Whitney U test for differences between control and each of cuff-implanted groups.

Axonal degeneration and fiber regeneration in the implanted nerves

In the control material, the myelinated fiber cross-sections had a regular appearance, with tightly packed myelin membrane and sporadically visible cytoplasm of Schwann cells with Schmidt-Lanterman notches. In the implanted rats, at the mid-point to a cuff electrode, in the most affected nerves (Xh5 NS,

Xh7 NS) there was a damage characterized by focal fiber loss. Areas filled with cellular debris and cells with the morphology of phagocytic macrophages were visible in the most changed sections (Fig. 7). Single ovoids and clusters of hypomyelinated (remyelinating) of 3 or more fibers were observed (Fig. 6B, 6C).

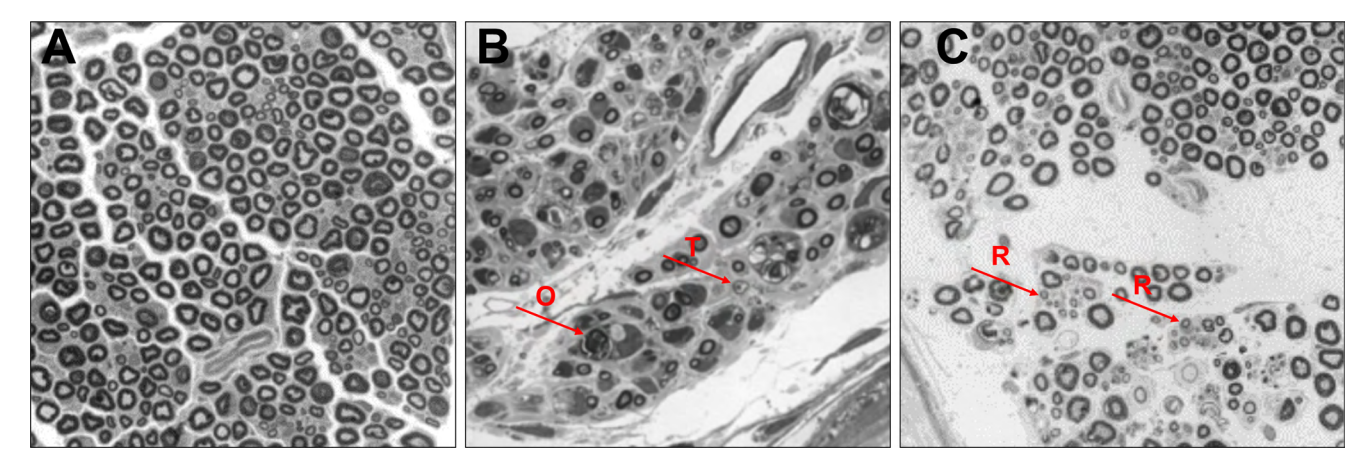


Fig. 7. Images of the rat tibial nerve (all from Xh5 NS sample) at the mid-point to a cuff electrode at 4 weeks post-implantation showing myelinated fibers. (A) Mixed peripheral nerves contain populations of large and small myelinated fibers (black rings). Unmyelinated fibers are not visible here. (B) Some nerves show diffuse loss of fibers with increased interfiber distances, possibly secondary to endoneurial edema, accompanied by thinly myelinated fibers (T) and ovoids (O). (C) Some small thinly myelinated fibers demonstrated features of hypomyelination indicative to remyelination (R).

Changes in the ultrastructure of myelinated axons, unmyelinated axon bundles and blood capillaries in the implanted nerves

The analysis of the ultrastructure was done with TEM on images collected from the endoneurium, perineurium and epineurium. The substantial observations are illustrated in Fig. 8 and Fig. 9.

In the endoneurium of the implanted nerves, the majority of myelinated axons did not show pathological features. Compact myelin laminae surrounded the axoplasm without signs of shrinkage (Fig. 8, Xh4, Xh8 nerves, NS and S). Fibers were surrounded by Schwann cells. In single axons (~15% per image; viewed at × 3000 and × 6000 magnification) axoplasm shrinkage occurred accompanied by myelin degradation products and sporadically by the subtle signs of myelin delamination (Fig. 8, bottom panel, white arrow). In the implanted nerves single mast cells were detected (Fig. 8, bottom panel). Macrophages, present sporadically in control material, were seen in the implanted nerves in regions with dispersed collagen fibers (exemplified in Fig. 8, Xh4S), and the activated fibroblasts occurred in the proximity of capillaries (Fig. 9).

Peripheral nerves contain multiple small-caliber non-myelinated axons which are ensheathed by non-myelinating Schwann cells (Remak Schwann cells, RSC, Fig. 8). In non-implanted nerves these axons were organized in bundles, densely packed, each axon surrounded by thin protrusions of centrally located RSC. In the implanted nerves some Remak bundles were loosely arranged, with thicker RSC protrusions separating them, and lower number of axons per bundle (exemplified by Xh4NS). In some implanted rats densely packed collagen fibers filling the intercellular spaces were separated by amorphous matrix suggesting that some shrinkage of the nerve occurred. That was particularly seen in the peripheral part of the endoneurium (not shown).

The blood vessels observed with TEM were elongated or oval, both in control and implanted nerves, of the diameter not exceeding 25 nanometers. In the capillary walls built of endothelial cells, their connections with tight junctions (TJ) and adherens junctions (AJ), were preserved in the majority of vessels in the implanted nerves (Fig. 9, middle panels). Basal membrane in control nerves demonstrated variable thickness, while in the majority of implanted nerves it was thin or moderate in the capillaries of the endoneurium and thicker in some capillaries in the epineurium. Sheets of extracellular matrix filling spaces between endothelial cells and pericytes were occasionally accompanied by activated fibroblasts and fibrous long spacing collagen produced by them. The secretory activity, assessed based

on the number of caveolae in the endothelial wall was maintained and directed mostly opposite to the vessel walls. We did not see differences in these features between NS and S nerves, what suggests that low-threshold stimulation of the tibial nerve does not change microanatomy of the nerve.

DISCUSSION

When undertaking our previous research (Gajewska-Woźniak et al., 2013) we considered the risks that chronic cuff electrodes over the posterior tibial nerve and intramuscular electrodes in the soleus muscle used in our experiments could affect the results observed in the H-reflex circuitry. There are indications that some compression of the nerve enwrapped for several months in the cuff-electrodes may cause damage affecting the most vulnerable large diameter Ia fibers (Stein et al., 1977b; Christian & Loeb, 1988). Stein and co-authors observed a small reduction in the number of large diameter fibers in the nerve enclosed over 9 months in the cuff electrode in cats (Stein et al., 1977b). In rats, the long-term (3-10 months after surgery) effects of electrodes implanted around the tibial nerve on the triceps surae (TS) motor units properties were reported to cause a small degree of muscle denervation with subsequent reinnervation (Carp et al., 2001). Our experiment lasted much shorter (4-5 weeks) limiting the probable compression effect in the cuff as this process requires time after implantation (Christian & Loeb, 1988). Still, our observation made on the increased levels of NT-3 neurotrophin and marked down-regulation of its high-affinity TrkC receptor transcripts, comparable in NS and S nerves (Gajewska-Woźniak et al., 2013), raised the questions on the condition of the nerve fibers and Schwann cells, dependent on the NT-3/TrkC signaling (Chen et al., 2002; Carrizosa et al., 2009; Mentis et al., 2010). Moreover, changes in NT-3 and BDNF protein levels and mRNA expression observed 28 days after mild compression of the sciatic nerve in the rats (Omura et al., 2005) were not matched by the changes observed in our study suggesting that chronic implantation of the cuff and intramuscular electrodes did not significantly affect the presented results. Drawing from these observations, to determine if degeneration and demyelination is occurring in our model we decided to examine the morphology of the tibial nerves from that study.

Within one month time frame of the current study, morphological changes resulting from the cuff nerve implantation and cuff maintenance were characterized by moderate shrinkage of the nerves, focal axon loss and demyelination, increased epineurial connective

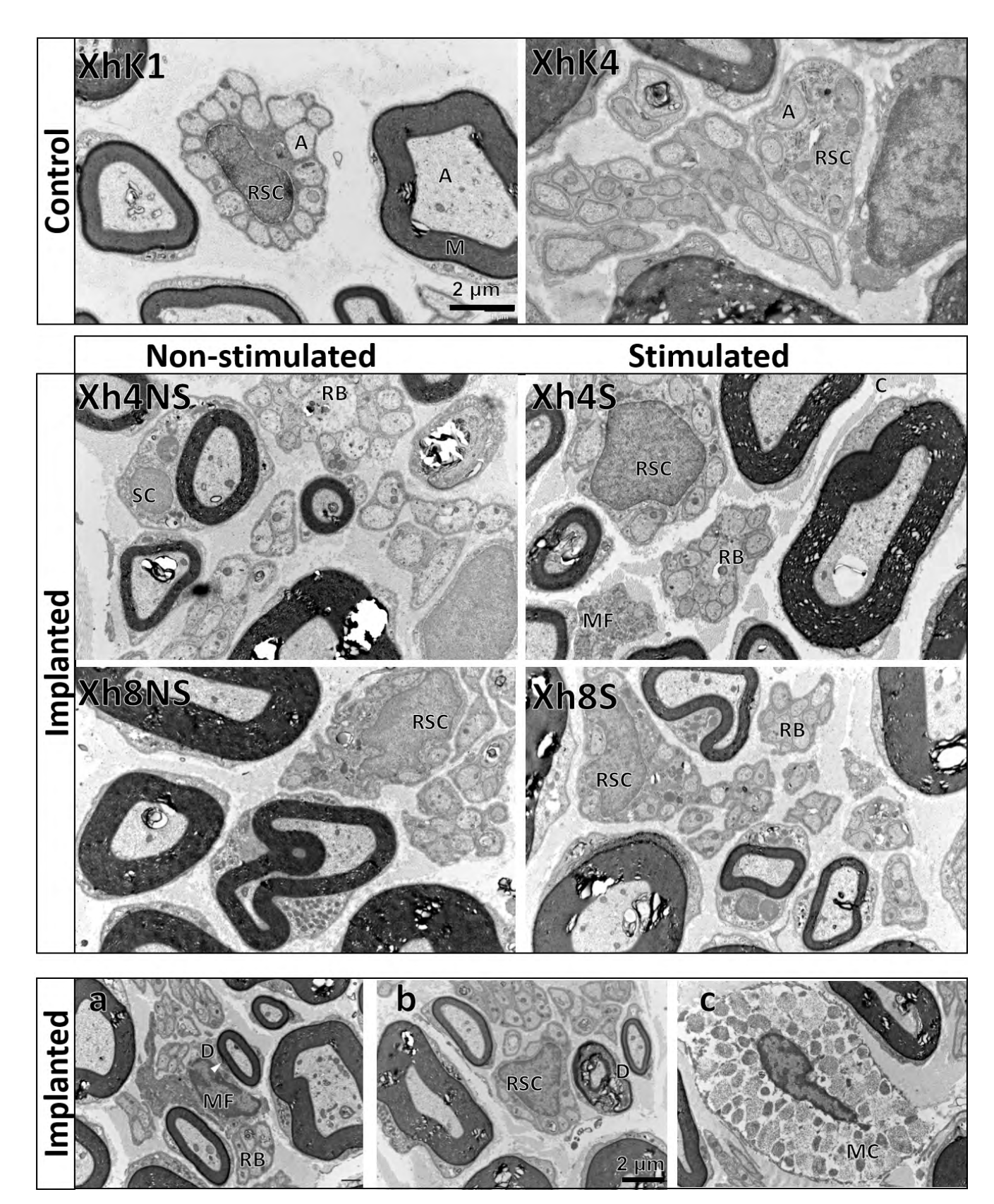


Fig. 8. Comparison of the organization of non-myelinated axons surrounded by non-myelinating Schwann cells (RSC), forming Remak bundles (RB) distributed between myelinated fibers. A – axon, M – myelin, D – demyelination, MF – macrophage, MC – mast cell. Images were taken from the central part of the endoneurium.

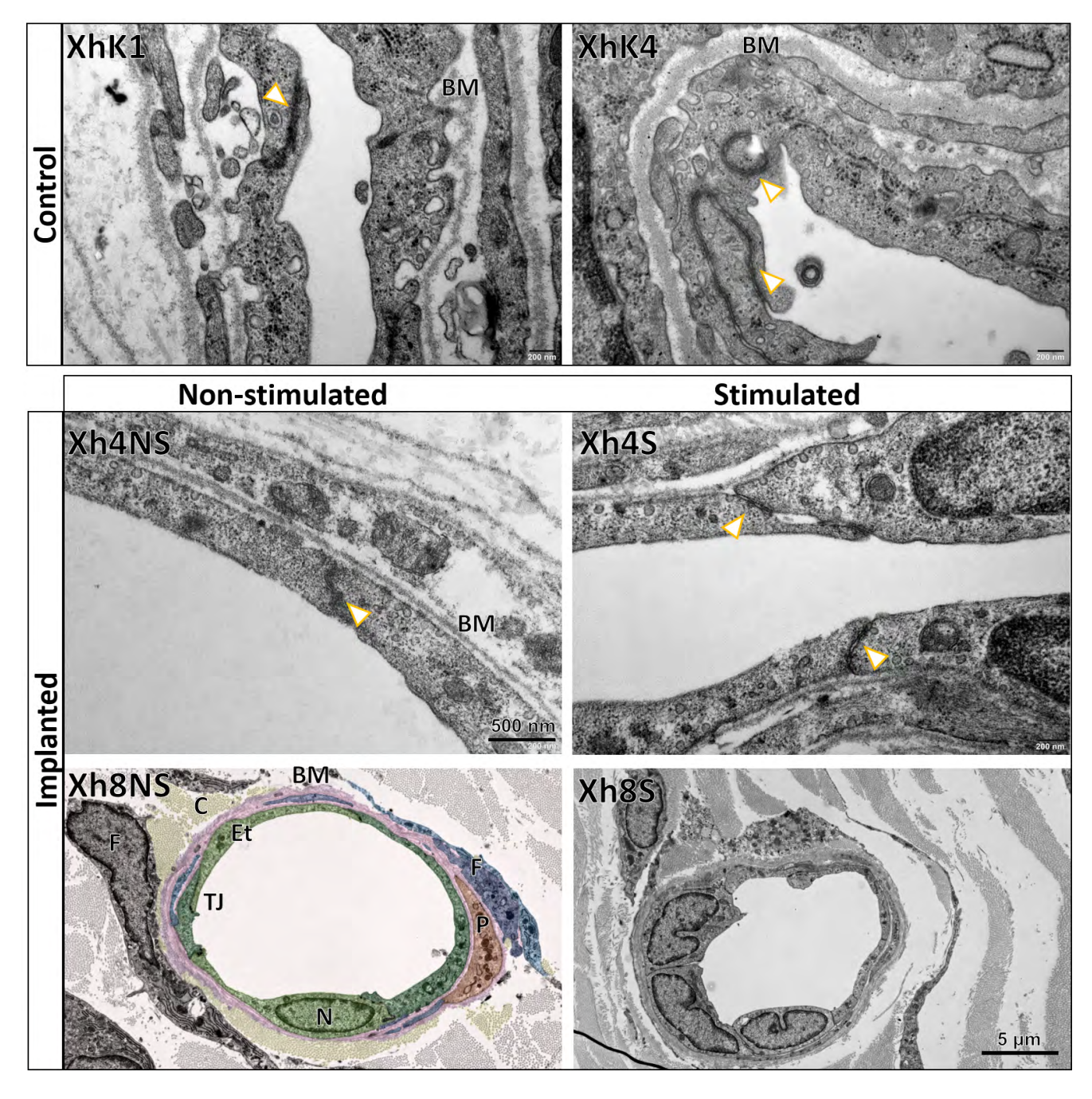


Fig. 9. Comparison of the structure of the capillary walls built of endothelial cells (Et) connected with tight junctions (TJ, arrows) and adherens junctions. Colored structures of the capillary from Xh8NS nerve mark endothelial cells (Et, green), pericyte (orange), basal membrane (BM, violet), fibroblasts (F, blue) and collagen fibers (C), a product of fibroblasts released to seal leaky capillary. Images from control and Xh4 rats were taken from the central part of the endoneurium. Images from Xh8 rat were taken from the epineurium.

tissue and occasional hypomyelinated (remyelinating) fibers, mostly detected on the periphery of the nerve. This form of damage (chronic, occurring over a period of four weeks), resembles that previously described for chronic peripheral nerve compression (Mackinnon et al., 1984) and was occasionally observed after helical

electrode implantation around the peroneal nerve in the cat (Agnew et al., 1989).

The frequency distribution of nerve fiber diameters measured in this study, together with their morphological appearance indicates, that implantation affects mostly large diameter, myelinated fibers. This observation draws attention to the fact that in the rat tibial nerve some axons are more vulnerable than others. That would suggest also that conduction by low-threshold proprioceptive Ia muscle afferents (the thickest fibers in the nerve) is impaired what may weaken effectiveness of the approach used, at least until restorative processes compensate functional deficit. Importantly to the knowledge on the recovery potential of the long-term implanted nerve, this study provides data on the growth of new sprouts and their myelination at one month from the surgery.

In our experiment, damage due to electrical stimulation with the selected parameters did not occur. Such damage, consisting of interstitial edema and early axonal degeneration was described after 7 days of prolonged high frequency stimulation of the peroneal nerve (8-16 hours 1.500 microampers, 100 Hz) (Agnew et al., 1989). A characteristic feature of such damage is a uniform distribution of degenerating fibers throughout the fascicles. In our study the distribution of degenerating axons was not uniform suggesting that the major component of the experimental procedure which causes moderate damage is the implantation itself.

Despite these risk factors our study shows that neither the presence of the electrode, nor the low-threshold stimulation of the nerve attenuated nerve ability to conduct currents from motor neurons to the muscles. Moreover, the potential to evoke the H-reflex mediated by Ia afferents was preserved (Gajewska-Woźniak et al., 2013). Assuming that lower number of VGLUT1 IF terminals apposing $\alpha\text{-LG MNs}$ in the sham-stimulated side, observed in those experiments, indicates some damage of Ia fibers in the tibial nerve, reversal of this effect in the stimulated hindlimb and current data indicate that successful functional recovery processes after stimulation of these afferents may occur at the level of nerve endings, without clear effect on axonal regeneration (Gajewska-Woźniak et al., 2016).

We made an observation of the enlargement of epineurium under the cuff. This outermost layer of dense irregular connective tissue surrounds multiple nerve fascicles as well as blood vessels which supply the nerve. In addition we detected multiple fibroblasts which contribute to the production of collagen fibers that form the backbone of the epineurium. Fibroblasts demonstrated activated phenotype, indicated by numerous, enlarged membranes of endoplasmic reticulum. We interpret these changes as providing structural support to the damaged fibers and functional support to the repair of the surrounding tissues.

One more aspect of nerve function after implantation and stimulation is the condition of small diameter, non-myelinating axons, organized by Remak Schwann cells into Remak bundles. Their morphology and orga-

nization, analyzed with TEM, allowed us to conclude that implantation had a mild effect on their organization which appeared slightly scattered in some areas, demonstrating control arrangement in other areas. Also screening of capillary vessel morphology provided data on preservation of tight junctions in majority of them, high level of transcytosis activity - as concluded from a high density of caveolae in the endothelial cytoplasm - and moderate widening of basal membrane. The latter suggests that in some areas of the endoneurium blood-nerve barrier permeability is increased as compared to the intact nerve.

CONCLUSION

In conclusion, because the stimulation proved effective in enrichment of motoneurons innervation the proposed approach can be considered beneficial therapeutically despite the accompanying risk of mild nerve injury, in particular with long-term electrode implantation.

ACKNOWLEDGEMENTS

This work received support from the Polish National Science Center grants 2013/09/B/NZ4/03306, 2018/31/B/NZ4/02789 and the Nencki Institute Statutory Grant. We appreciate Dr Hanna Drac from the Department of Neurology, Medical University of Warsaw, Poland, for her expertise in histopathological assessment of nerve preparations, and prof. Małgorzata Frontczak-Baniewicz for her expertise in transmission electron microscopy images interpretation.

TEM imaging was performed at the Laboratory of Electron Microscopy, which serves as an imaging core facility at the Nencki Institute of Experimental Biology and is part of the infrastructure of the Polish Euro-BioImaging Node. Polish Node is supported by the project co-financed by the Minister of Education and Science based on contract No 2022/WK/05 (Polish Euro-BioImaging Node "Advanced Light Microscopy Node Poland.

REFERENCES

Agnew, W. F., McCreery, D. B., Yuen, T. G. H., & Bullara, L. A. (1989). Histologic and physiologic evaluation of electrically stimulated peripheral nerve: Considerations for the selection of parameters. *Annals of Biomedical Engineering*, *17*(1), 39–60. https://doi.org/10.1007/BF02364272

Alvarez, F. J., Titus-Mitchell, H. E., Bullinger, K. L., Kraszpulski, M., Nardelli, P., & Cope, T. C. (2011). Permanent central synaptic disconnection of proprioceptors after nerve injury and regeneration. I. Loss

- of VGLUT1/IA synapses on motoneurons. *Journal of Neurophysiology*, 106(5), 2450–2470. https://doi.org/10.1152/jn.01095.2010
- Badia, J., Pascual-Font, A., Vivó, M., Udina, E., & Navarro, X. (2010). Topographical distribution of motor fascicles in the sciatic-tibial nerve of the rat. *Muscle & Nerve*, *42*(2), 192–201. https://doi.org/10.1002/mus.21652
- Carp, J. S., Chen, X. Y., Sheikh, H., & Wolpaw, J. R. (2001). Effects of chronic nerve cuff and intramuscular electrodes on rat triceps surae motor units. *Neuroscience Letters*, *312*(1), 1–4. https://doi.org/10.1016/s0304-3940(01)02183-8
- Carrizosa, M. A. D.-L. de, Morado-Díaz, C. J., Tena, J. J., Benítez-Temiño, B., Pecero, M. L., Morcuende, S. R., Cruz, R. R. de la, & Pastor, A. M. (2009). Complementary Actions of BDNF and Neurotrophin-3 on the Firing Patterns and Synaptic Composition of Motoneurons. *Journal of Neuroscience*, 29(2), 575–587. https://doi.org/10.1523/ JNEUROSCI.5312-08.2009
- Chen, H.-H., Tourtellotte, W. G., & Frank, E. (2002). Muscle Spindle-Derived Neurotrophin 3 Regulates Synaptic Connectivity between Muscle Sensory and Motor Neurons. *Journal of Neuroscience*, *22*(9), 3512–3519. https://doi.org/10.1523/JNEUROSCI.22-09-03512.2002
- Chen, X. Y., Chen, Y., Wang, Y., Thompson, A., Carp, J. S., Segal, R. L., & Wolpaw, J. R. (2010). Reflex conditioning: A new strategy for improving motor function after spinal cord injury. *Annals of the New York Academy of Sciences*, 1198(s1), E12–E21. https://doi.org/10.1111/j.1749-6632.2010.05565.x
- Chen, Y., Chen, L., Wang, Y., Wolpaw, J. R., & Chen, X. Y. (2014). Persistent beneficial impact of H-reflex conditioning in spinal cord-injured rats. *Journal of Neurophysiology*, 112(10), 2374–2381. https://doi.org/10.1152/ in.00422.2014
- Chen, Y., Chen, X. Y., Jakeman, L. B., Chen, L., Stokes, B. T., & Wolpaw, J. R. (2006). Operant Conditioning of H-Reflex Can Correct a Locomotor Abnormality after Spinal Cord Injury in Rats. *Journal of Neuroscience*, 26(48), 12537–12543. https://doi.org/10.1523/JNEUROSCI.2198-06.2006
- Chen, Y., Wang, Y., Chen, L., Sun, C., English, A. W., Wolpaw, J. R., & Chen, X. Y. (2010). H-Reflex Up-Conditioning Encourages Recovery of EMG Activity and H-Reflexes after Sciatic Nerve Transection and Repair in Rats. *The Journal of Neuroscience*, *30*(48), 16128–16136. https://doi.org/10.1523/JNEUROSCI.4578-10.2010
- Christian, K., & Loeb, G. E. (1988). Conduction studies in peripheral cat nerve using implanted electrodes: I. Methods and findings in controls. *Muscle & Nerve*, 11(9), 922–932. https://doi.org/10.1002/mus.880110905
- Czarkowska, J., Jankowska, E., & Sybirska, E. (1976). Axonal projections of spinal interneurones excited by group I afferents in the cat, revealed by intracellular staining with horseradish peroxidase. *Brain Research*, *118*(1), 115–118. https://doi.org/10.1016/0006-8993(76)90844-1
- Fisher, L. E., Ayers, C. A., Ciollaro, M., Ventura, V., Weber, D. J., & Gaunt, R. A. (2014). Chronic recruitment of primary afferent neurons by microstimulation in the feline dorsal root ganglia. *Journal of Neural Engineering*, *11*(3), 036007. https://doi.org/10.1088/1741-2560/11/3/036007
- Gajewska-Woźniak, O., Grycz, K., Czarkowska-Bauch, J., & Skup, M. (2016). Electrical Stimulation of Low-Threshold Proprioceptive Fibers in the Adult Rat Increases Density of Glutamatergic and Cholinergic Terminals on Ankle Extensor α-Motoneurons. *PloS One, 11*(8), e0161614. https://doi.org/10.1371/journal.pone.0161614
- Gajewska-Woźniak, O., Skup, M., Kasicki, S., Ziemlińska, E., & Czarkowska-Bauch, J. (2013). Enhancing Proprioceptive Input to Motoneurons Differentially Affects Expression of Neurotrophin 3 and Brain-Derived Neurotrophic Factor in Rat Hoffmann-Reflex Circuitry. PLOS ONE, 8(6), e65937. https://doi.org/10.1371/journal.pone.0065937
- Grycz, K., Głowacka, A., Ji, B., Czarkowska-Bauch, J., Gajewska-Woźniak, O., & Skup, M. (2019). Early pre- and postsynaptic decrease in glutamatergic

- and cholinergic signaling after spinalization is not modified when stimulating proprioceptive input to the ankle extensor α -motoneurons: Anatomical and neurochemical study. *PLOS ONE*, *14*(9), e0222849. https://doi.org/10.1371/journal.pone.0222849
- Loeb, G. E., & Peck, R. A. (1996). Cuff electrodes for chronic stimulation and recording of peripheral nerve activity. *Journal of Neuroscience Methods*, 64(1), 95–103. https://doi.org/10.1016/0165-0270(95)00123-9
- Mackinnon, S. E., Dellon, A. L., Hudson, A. R., & Hunter, D. A. (1984). Chronic nerve compression—An experimental model in the rat. *Annals of Plastic Surgery*, *13*(2), 112–120. https://doi.org/10.1097/00000637-198408000-00004
- Mendell, L. M., Johnson, R. D., & Munson, J. B. (1999). Neurotrophin modulation of the monosynaptic reflex after peripheral nerve transection. *The Journal of Neuroscience: The Official Journal of the Society for Neuroscience*, 19(8), 3162–3170. https://doi.org/10.1523/JNEUROSCI.19-08-03162.1999
- Mentis, G. Z., Alvarez, F. J., Shneider, N. A., Siembab, V. C., & O'Donovan, M. J. (2010). Mechanisms regulating the specificity and strength of muscle afferent inputs in the spinal cord. *Annals of the New York Academy of Sciences*, 1198, 220–230. https://doi.org/10.1111/j.1749-6632.2010.05538.x
- Ochoa, J., Danta, G., Fowler, T. J., & Gilliatt, R. W. (1971). Nature of the Nerve Lesion caused by a Pneumatic Tourniquet. *Nature*, *233*(5317), 265–266. https://doi.org/10.1038/233265a0
- Omura T., Sano M., Omura K., Hasegawa T., Doi M., et al. (2005) Different expressions of BDNF, NT3, and NT4 in muscle and nerve after various types of peripheral nerve injuries. J Peripheral Nervous System 10: 293–300.
- Reina, M. A., Arriazu, R., Collier, C. B., Sala-Blanch, X., Izquierdo, L., & de Andrés, J. (2013). Electron microscopy of human peripheral nerves of clinical relevance to the practice of nerve blocks. A structural and ultrastructural review based on original experimental and laboratory data. *Revista Española de Anestesiología y Reanimación*, 60(10), 552–562. https://doi.org/10.1016/j.redar.2013.06.006
- Reina, M. A., & Sala-Blanch, X. (2015). Ultrastructure of the Epineurium. In M. A. Reina, J. A. De Andrés, A. Hadzic, A. Prats-Galino, X. Sala-Blanch, & A. A. J. van Zundert (Eds.), Atlas of Functional Anatomy for Regional Anesthesia and Pain Medicine: Human Structure, Ultrastructure and 3D Reconstruction Images (pp. 85–98). Springer International Publishing. https:// doi.org/10.1007/978-3-319-09522-6_5
- Rydevik, B., & Lundborg, G. (1977). Permeability of intraneural microvessels and perineurium following acute, graded experimental nerve compression. *Scandinavian Journal of Plastic and Reconstructive Surgery*, *11*(3), 179–187. https://doi.org/10.3109/02844317709025516
- Sauter, J. F., Niijima, A., Berthoud, H. R., & Jeanrenaud, B. (1983). Vagal neurons and pathways to the rat's lower viscera: An electrophysiological study. *Brain Research Bulletin*, *11*(5), 487–491. https://doi.org/10.1016/0361-9230(83)90119-3
- Schmalbruch, H. (1986). Fiber composition of the rat sciatic nerve. *The Anatomical Record*, 215(1), 71–81. https://doi.org/10.1002/ar.1092150111
- Stein, R. B., Nichols, T. R., Jhamandas, J., Davis, L., & Charles, D. (1977a). Stable long-term recordings from cat peripheral nerves. *Brain Research*, 128(1), 21–38. https://doi.org/10.1016/0006-8993(77)90233-5
- Stein, R. B., Nichols, T. R., Jhamandas, J., Davis, L., & Charles, D. (1977b). Stable long-term recordings from cat peripheral nerves. *Brain Research*, 128(1), 21–38. https://doi.org/10.1016/0006-8993(77)90233-5
- Szabolcs, M. J., Windisch, A., Koller, R., & Pensch, M. (1991). Axon typing of rat muscle nerves using a double staining procedure for cholinesterase and carbonic anhydrase. *The journal of histochemistry and cytochemistry*, 39(12), 1617–1625. https://doi.org/10.1177/39.12.1719070